Nonequilibrium kinetics of a radiative CO flow behind a shock wave

A. Aliat and A. Chikhaoui
IUSTI, Université de Provence, 5, Rue E. Fermi, 13453 Marseille Cedex 13, France

E. V. Kustova
Department of Mathematics and Mechanics, Saint Petersburg University, 198504, Universitetski Prospekt 28, Saint Petersburg, Russia

(Received 14 July 2003; published 20 November 2003)

An investigation is presented of a highly nonequilibrium CO flow with consistently coupled vibrational energy exchanges, chemical reactions, and radiation. A detailed state-to-state model taking into account vibration-vibration, vibration-translation, and vibration-electronic transitions, dissociation-recombination reactions, and radiative transitions between vibrational and electronic states is developed on the basis of kinetic theory methods. A closed set of master equations for vibration-electronic level populations, number densities of atomic species, radiation intensity, temperature, and velocity is derived, and a one-dimensional inviscid carbon monoxide flow behind a plane shock wave is studied numerically. Several models of vibrational transition and dissociation rates in high temperature carbon monoxide are tested, and a model satisfying both accuracy and feasibility requirements is recommended. The role of various energy transfers and chemical reactions in the formation of nonequilibrium vibrational distributions in a shock heated CO flow is studied, and the influence of state-to-state distributions on macroscopic flow parameters and radiation intensity is discussed.

DOI: 10.1103/PhysRevE.68.056306 PACS number(s): 47.70.−n, 44.40.+a, 51.10.+y, 82.20.Rp

I. INTRODUCTION

Nonequilibrium carbon monoxide kinetics has been widely discussed in the literature for many years because of its importance for applications: molecular lasers, environmental problems, planetary atmosphere exploration. The kinetics of electrical discharges and optically pumped CO has been investigated thoroughly during the last two decades (see [1–9]). As a result, in pumped systems with high vibrational energy storage, essentially non-Boltzmann vibrational distributions have been found both experimentally and by means of state-to-state calculations. At the same time, although some experimental results on CO kinetics in shock tubes are available in the literature [10–13], the peculiarities of vibration-chemical kinetics in shock heated CO are not yet completely known. The majority of theoretical models are based on quasistationary distributions over vibrational energies. Quasistationary multitemperature models are valid under the assumption that characteristic times of vibration-vibration (VV) and vibration-translation (VT) relaxation and chemical reactions differ by many orders of magnitude. However, accurate calculations of VV and VT exchange rates [14–17] as well as dissociation rates [17,18] show that the validity of this assumption is limited, and in a wide temperature range these characteristic times cannot be distinguished. That is why for better understanding of nonequilibrium CO kinetics behind shock waves a more detailed state-to-state approach should be applied.

The main advantage of the state-to-state approach is that it is not based on any quasi-stationary (Boltzmann or Treanor) distribution over vibrational energy and therefore can predict correctly the behavior of vibrational level populations. This is the reason for the rapid development of this method for the investigation of reacting gas flows. Recently, many various flows have been studied using this approach: high temperature N_2 and O_2 flows behind shock waves [19–21], expanding flows in nozzles [22–25], flows in boundary layers [26,27], and near blunt bodies [28]. Transport kinetic theory in the state-to-state approach was developed in [29], and the results of [30–32] show a significant influence of nonequilibrium vibrational distributions on the heat transfer. However, a consistent coupling of vibration-electronic energy exchanges and radiation in real gas flows and a thorough study of the radiative heat transfer in the state-to-state approach have not yet been performed. Although equations of aerothermochemistry taking into account radiative effects have been considered by many authors [33–37], they are usually based on the local thermal equilibrium (LTE) assumption, i.e., the existence of a one-temperature thermal equilibrium Boltzmann distribution over vibrational energy is assumed. This hypothesis can lead to significant errors in the estimated values of the radiative heat flux from strongly nonequilibrium flow regions. Accurate evaluation of the heat transfer caused by radiation is of importance for many modern applications, in particular, in reentry problems and the design of thermal protection systems.

A general state-to-state kinetic model of a nonequilibrium flow taking into account the coupling of vibrational relaxation, chemical reactions, and radiation was developed in [38], and in [39] this model was extended to take into account vibration-electronic (VE) energy transfers as well as radiative transitions from electronically excited states. In the present paper the approach presented in [38,39] is applied for the simulation of a nonequilibrium one-dimensional inviscid carbon monoxide flow behind a plane shock wave. The contribution of various energy transfers to the formation of vibrational distributions, and their influence on macroscopic flow parameters and radiation intensity are studied. Different models for the rates of vibrational transitions and dissociation are considered, and the choice of an appropriate model is discussed.

II. KINETIC MODEL

In Refs. [38–40], a nonequilibrium gas flow is described on the basis of kinetic equations for distribution functions. Distribution functions for material particles $f_{c\alpha ij}(\mathbf{r},\mathbf{p}_c,t)$ are introduced for chemical species c, electronic state α, and vibrational and rotational energy levels i and j, respectively (t is the time, and $\mathbf{r}$ and $\mathbf{p}$ are the spatial coordinates and momentum). For photons $f_\nu(\mathbf{r},\mathbf{p}_\nu,t)$ are defined for each frequency ν.

Kinetic equations for distribution functions of material particles can be expressed in terms of the microscopic particle velocity $\mathbf{u}_c$:

$$\frac{\partial f_{c\alpha ij}}{\partial t}+\mathbf{u}_c\cdot\frac{\partial f_{c\alpha ij}}{\partial \mathbf{r}}=J_{c\alpha ij}, \tag{1}$$

whereas for the distribution function of photons the equations are written in terms of the momentum:

$$\frac{\partial f_\nu}{\partial t}+c\boldsymbol{\Omega}_\nu\cdot\frac{\partial f_\nu}{\partial \mathbf{r}}=J_\nu, \tag{2}$$

where $\boldsymbol{\Omega}_\nu$ is the unit vector defining the direction of travel of the photon, and c is the speed of light. The collision operators $J_{c\alpha ij}$ and J_ν describe all collisions leading to the change of distribution functions

$$J_{c\alpha ij}=J^{el}_{c\alpha ij}+J^{inel}_{c\alpha ij}+J^{react}_{c\alpha ij}+J^{rad}_{c\alpha ij},$$

$$J_\nu=J^{rad}_\nu=J^{em}_\nu+J^{abs}_\nu.$$

$J^{el}_{c\alpha ij}$ and $J^{inel}_{c\alpha ij}$ are the operators of elastic and inelastic collisions, $J^{react}_{c\alpha ij}$ describes chemically reactive collisions, $J^{rad}_{c\alpha ij}=J^{em}_{c\alpha ij}+J^{abs}_{c\alpha ij}$ corresponds to radiative transitions including absorption and induced and spontaneous emission (scattering of photons is neglected in this study). Among inelastic collisions one can distinguish inelastic rotation-translation (RT) exchanges, VT transitions, VV exchanges, and VE transitions. Consequently, the integral operator $J^{inel}_{c\alpha ij}$ can be presented in the form

$$J^{inel}_{c\alpha ij}=J^{RT}_{c\alpha ij}+J^{VT}_{c\alpha ij}+J^{VV}_{c\alpha ij}+J^{VE}_{c\alpha ij}.$$

Since the work of Wang Chang and Uhlenbeck [41] and Ludwig and Heil [42], integral operators of collisions between material particles have been obtained by many authors and are summarized in [38,43]. Expressions for $J^{rad}_{c\alpha ij}, J^{rad}_\nu$ were derived in [38,39].

It is well known that relaxation times of translational and rotational degrees of freedom are much shorter than the vibrational relaxation time and characteristic times of chemical reactions and radiation:

$$\tau_{el}\sim\tau_{RT}\ll\tau_{VV}\sim\tau_{VT}\sim\tau_{VE}\sim\tau_{react}\sim\tau_{rad}\sim\theta \tag{3}$$

(τ_{el}, τ_{RT}, τ_{VV}, τ_{VT}, τ_{VE}, τ_{react}, τ_{rad} are the characteristic times of the corresponding processes, and θ is the mean time of macroscopic parameter change). Under condition (3), Eqs. (1) and (2) in dimensionless form can be written as

$$\frac{\partial f_{c\alpha ij}}{\partial t}+\mathbf{u}_c\cdot\frac{\partial f_{c\alpha ij}}{\partial \mathbf{r}}=\frac{1}{\epsilon}J^{rap}_{c\alpha ij}+J^{sl}_{c\alpha ij}, \tag{4}$$

$$\frac{\partial f_\nu}{\partial t}+c\boldsymbol{\Omega}_\nu\cdot\frac{\partial f_\nu}{\partial \mathbf{r}}=J^{rad}_\nu. \tag{5}$$

Here $\epsilon\sim\tau_{el}/\theta$ is a small parameter. The collision operators of rapid and slow processes under condition (3) include the following terms:

$$J^{rap}_{c\alpha ij}=J^{el}_{c\alpha ij}+J^{RT}_{c\alpha ij}, \tag{6}$$

$$J^{sl}_{c\alpha ij}=J^{VV}_{c\alpha ij}+J^{VT}_{c\alpha ij}+J^{VE}_{c\alpha ij}+J^{react}_{c\alpha ij}+J^{rad}_{c\alpha ij}. \tag{7}$$

The solution of Eqs. (4), using the Chapman-Enskog method generalized for highly nonequilibrium flows with rapid and slow processes [38,43] can be sought as an expansion of $f_{c\alpha ij}$ in a power series of ϵ. The zero-order distribution function of material particles is determined by collision invariants of the most rapid processes (whose characteristic times are much smaller compared to θ), and has been found in the form

$$f^{(0)}_{c\alpha ij}=\left(\frac{m_c}{2\pi kT}\right)^{3/2}\frac{n_{c\alpha i}s^{c\alpha i}_j}{Z^{c\alpha i}_{rot}}\exp\left(-\frac{m_cC_c^2}{2kT}-\frac{\varepsilon^{c\alpha i}_j}{kT}\right), \tag{8}$$

where m_c is the molecular mass, k is the Boltzmann constant, T is the gas temperature, $n_{c\alpha i}$ is the number density of molecules of c species at the internal state (α,i), $\mathbf{C}_c=\mathbf{u}_c-\mathbf{v}$ is the peculiar velocity ($\mathbf{v}$ is the macroscopic gas velocity), $s^{c\alpha i}_j$ and $\varepsilon^{c\alpha i}_j$ are, respectively, the rotational statistic weight and rotational energy in the corresponding electronic and vibrational state, and $Z^{c\alpha i}_{rot}$ is the rotational partition function. The distribution function (8) represents the local equilibrium Maxwell-Boltzmann distribution over velocities and rotational energies and the strongly nonequilibrium distribution over vibrational energies and chemical species. It is expressed in terms of the macroscopic parameters $n_{c\alpha i}(\mathbf{r},t)$, $\mathbf{v}(\mathbf{r},t)$, and $T(\mathbf{r},t)$. As no quasistationary vibrational distributions $n_{c\alpha i}(T)$ exist, vibrational and electronic state populations are found by solving the equations of detailed state-to-state vibrational-chemical kinetics. A closed system of macroscopic equations for $n_{c\alpha i}$, $\mathbf{v}$, and T in the zero-order approximation is given in the next section for a one-dimensional steady state flow.

The change of the photon distribution proceeds at the time scale $\tau\sim\theta$ and therefore the distribution functions of photons f_ν can be found directly from microscopic equations (5). It is conventional to introduce the specific intensity I_ν of the radiation field

$$I_\nu d\nu d\boldsymbol{\Omega}_\nu=ch\nu f_\nu d\mathbf{p}_\nu, \tag{9}$$

where h is the Planck constant, and ν is the frequency. Then Eqs. (5) can be rewritten in the form of equations of radiative transfer:

$$\frac{1}{c}\frac{\partial I_\nu}{\partial t}+\mathbf{\Omega}_\nu\cdot\frac{\partial I_\nu}{\partial \mathbf{r}}=\frac{h^4\nu^3}{c^3}J_\nu^{rad}. \tag{10}$$

First-order distribution functions of material particles and macroscopic equations in the state-to-state approach were obtained in [29,38,39]. The first-order transport terms were investigated thoroughly in [29]. In particular, it was shown that the heat flux is determined by gradients of the temperature and nonequilibrium populations $n_{c\alpha i}$, and thus depends essentially on state-to-state vibrational distributions. In the present paper, an inviscid gas flow is studied and therefore first-order transport terms are not considered.

III. MACROSCOPIC EQUATIONS

A closed system of macroscopic equations for the parameters $n_{c\alpha i}(\mathbf{r},t)$, $\mathbf{v}(\mathbf{r},t)$, $T(\mathbf{r},t)$, and $I_\nu(\mathbf{r},t)$ in the general form was derived from the kinetic equations in [38,39]. This system consists of the equations of detailed state-to-state vibration-chemical kinetics for $n_{c\alpha i}$, conservation of momentum and total energy, and the equations of radiative transfer.

In this paper, a steady state one-dimensional inviscid CO flow behind a plane shock wave is studied. It is assumed that a mixture is constituted of CO molecules in the ground electronic state $X\ ^1\Sigma$ and excited electronic states $a\ ^3\Pi$ and $A\ ^1\Pi$, and of carbon and oxygen atoms C and O. In this case, the system of macroscopic equations reads

$$\frac{d(vn_{\alpha i})}{dx}=R_{\alpha i},\quad \alpha=1,2,3,\quad i=0,\ldots,L_\alpha, \tag{11}$$

$$\frac{d(vn_{\mathrm{C}})}{dx}=\frac{d(vn_{\mathrm{O}})}{dx}=R_{at}^{react}, \tag{12}$$

$$\rho v\frac{dv}{dx}+\frac{dp}{dx}=0, \tag{13}$$

$$\rho v\frac{dU}{dx}+\frac{dq_{rad}}{dx}+p\frac{dv}{dx}=0, \tag{14}$$

$$\frac{dI_\nu}{dx}=R_\nu^{rad}, \tag{15}$$

where x is the direction of the shock wave propagation, v is the flow velocity in the x direction, $n_{\alpha i}$ is the population of the ith molecular vibrational level of the electronic state α, L_α is the number of excited vibrational levels for the corresponding electronic state, n_{C} and n_{O} are the number densities of C and O atoms, $p=nkT$ is the pressure, ρ is the density, U is the total energy of material particles per unit mass (U depends on the temperature and all $n_{c\alpha i}$), and the production terms in Eqs. (11) and (12) are determined by the collision operator of all slow processes and the operator of chemical reactions with atom formation, respectively:

$$R_{\alpha i}=\sum_j\int J_{\alpha ij}^{sl}d\mathbf{u}_c, \tag{16}$$

$$R_{at}^{react}=-\sum_{\alpha ij}\int J_{\alpha ij}^{react}d\mathbf{u}_c. \tag{17}$$

The radiative heat flux $\mathbf{q}_{rad}$ is given by the formula

$$\mathbf{q}_{rad}=\int_0^\infty\int_{4\pi}I_\nu\mathbf{\Omega}_\nu d\nu d\mathbf{\Omega}_\nu \tag{18}$$

and can be found directly using the solution of the equations of radiative transfer (10) [38]. Note that in the inviscid approximation the diffusion velocity and heat flux by material particles vanish as a result of the Maxwellian distribution over velocities. However, the radiative flux $\mathbf{q}_{rad}$ cannot be removed from Eq. (14) in the Euler approximation, because it is determined by the microscopic distribution function of photons, which does not depend on the order of approximation of the asymptotic method.

In order to write explicitly the production terms in Eqs. (11), (12), and (15) it is necessary to specify the set of energy transitions and chemical reactions which contribute to slow processes. Vibrational energy transitions included to the reaction scheme are as follows: VV exchanges of vibrational quanta between CO molecules,

$$\mathrm{CO}(i)+\mathrm{CO}(k)\rightleftharpoons\mathrm{CO}(i')+\mathrm{CO}(k'); \tag{19}$$

VT transitions (M states for CO, C, or O),

$$\mathrm{CO}(i)+M\rightleftharpoons\mathrm{CO}(i')+M; \tag{20}$$

and near-resonant VE exchanges,

$$\mathrm{CO}(X\ ^1\Sigma,i\sim27)+M\rightarrow\mathrm{CO}(a\ ^3\Pi,i\sim0)+M; \tag{21}$$

$$\mathrm{CO}(X\ ^1\Sigma,i\sim40)+M\rightarrow\mathrm{CO}(A\ ^1\Pi,i\sim0)+M. \tag{22}$$

The VE transitions (21) and (22) from high vibrational levels to approximately isoenergetic excited electronic states are known to be important in the optically pumped systems [5,6,8,9]. One of the objectives of the present study is to check the role of these transitions in the kinetics of shock heated CO.

The chemical reaction scheme, at this stage, includes only dissociation and recombination of CO molecules:

$$\mathrm{CO}+M\rightleftharpoons\mathrm{C}+\mathrm{O}+M. \tag{23}$$

It should be noted that in high temperature CO flows reactions leading to O_2 and C_2 formation also take place. However, it is shown in [10] that reactions producing O_2,

$$\mathrm{O}+\mathrm{CO}\rightleftharpoons\mathrm{O_2}+\mathrm{C}, \tag{24}$$

$$\mathrm{O}+\mathrm{O}+M\rightleftharpoons\mathrm{O_2}+M, \tag{25}$$

contribute very weakly to CO kinetics in shock tube experiments. On the other hand, C_2 formation through the reactions

$$\mathrm{C}+\mathrm{CO}\rightleftharpoons\mathrm{C_2}+\mathrm{O}, \tag{26}$$

$$\mathrm{C}+\mathrm{C}+M\rightleftharpoons\mathrm{C_2}+M \tag{27}$$

can play an important role in high temperature conditions. Indeed, in shock tube experiments [10] the radiation of the C_2 Swan band ($d\ ^3\Pi \rightarrow a\ ^3\Pi$) has been observed. Nevertheless, this study is limited by the conditions when the degree of CO dissociation is low and therefore the concentration of C atoms contributing to reactions (26) and (27) is not sufficiently high to produce a noticeable amount of C_2. Including reactions (26) and (27) in the kinetic scheme represents an important perspective for the investigation of high temperature CO flows.

Two ranges of radiative transitions are considered: (1) ir radiation due to transitions between vibrational states, and (2) uv and visible radiation caused by transitions between electronic states. The most intensive band observed in the uv and visible range is the CO fourth positive band (the responsible transition is $A\ ^1\Pi \rightarrow X\ ^1\Sigma$).

Among radiative transitions, the induced emission and absorption

$$\mathrm{CO}(\alpha,i)+h\nu \rightleftharpoons \mathrm{CO}(\alpha',i')+2h\nu \tag{28}$$

and spontaneous emission

$$\mathrm{CO}(\alpha,i)\rightarrow \mathrm{CO}(\alpha',i')+h\nu \tag{29}$$

are distinguished.

Now let us write the production terms. The total production term in Eq. (11) represents the sum of several terms responsible for various processes:

$$R_{\alpha i}=R_{\alpha i}^{VV}+\sum_M (R_{\alpha i}^{VT,\ M}+R_{\alpha i}^{VE,\ M}+R_{\alpha i}^{react,\ M})+R_{\alpha i}^{rad}, \tag{30}$$

where $M=\mathrm{CO}$, C, O, and

$$R_{\alpha i}^{VV}=\sum_k \sum_{k'\neq k} \sum_{i'\neq i} (k_{\alpha,\ i'i}^{k'k} n_{\alpha i'} n_{\alpha k'} - k_{\alpha,\ ii'}^{kk'} n_{\alpha i} n_{\alpha k}), \tag{31}$$

$$R_{\alpha i}^{VT,\ M}=n_M \sum_{i'\neq i} (k_{\alpha,\ i'i}^{M} n_{\alpha i'} - k_{\alpha,\ ii'}^{M} n_{\alpha i}), \tag{32}$$

$$R_{\alpha i}^{VE,\ M}=n_M \sum_{\alpha'\neq \alpha} \sum_{i'} (k_{\alpha' i'\alpha i}^{M} n_{\alpha' i'} - k_{\alpha i\alpha' i'}^{M} n_{\alpha i}), \tag{33}$$

$$R_{\alpha i}^{react,\ M}=R_{\alpha i}^{diss,\ M}=n_M (k_{rec,\alpha i}^{M} n_C n_O - k_{\alpha i,diss}^{M} n_{\alpha i}). \tag{34}$$

Here $k_{\alpha,\ ii'}^{kk'}$ are the rate coefficients for $(i,k\rightarrow i',k')$ vibrational energy exchanges between two molecules in the same electronic states; $k_{\alpha,\ ii'}^{M}$ and $k_{\alpha i\alpha' i'}^{M}$ are the rate coefficients for VT $(i\rightarrow i')$ and VE $(\alpha i\rightarrow \alpha' i')$ energy transitions in a collision with a partner M; $k_{rec,\alpha i}^{M}$ are the state-to-state rate coefficients of recombination to the ith level of the electronic state α; $k_{\alpha i,diss}^{M}$ are the rate coefficients of dissociation from the ith level of the electronic state α.

Modeling of the rate coefficients for vibrational energy exchanges and dissociation has remained the focus of attention in recent decades. There exist some low temperature experimental data on the VV and VT energy transfer in carbon monoxide [4,44], which show that for CO molecules taking into account both long-range and short-range forces is of particular importance. Exact quantum trajectory calculations of rate coefficients for vibrational transitions have been performed by several authors [14–17,45]. One of the commonly used analytical approaches is the semiclassical first-order perturbation Schwartz-Slawsky-Herzfeld (SSH) theory [46], its generalization for anharmonic oscillators is given in [47]. It works rather well for low quantum states while at high collision velocities and for high quantum numbers it fails. A more rigorous analytical nonperturbative semiclassical forced harmonic oscillator (FHO) model elaborated in [21] gives rather accurate values for probabilities of VV and VT transitions (including multiquantum jumps). Unfortunately, the direct use of trajectory methods and complete FHO model in computational fluid dynamics (CFD) codes is hardly possible due to their complexity, and therefore some time saving approximations are required for numerical simulations. For this purpose, interpolations of experimental measurements or quantum calculations can be used. One can find some interpolating formulas of trajectory results [14,15] for N_2 and O_2 (see [27]), but for CO no fitting has been done. In Ref. [4] semiempirical formulas for the rate coefficients of VV and VT energy exchanges are given in a form similar to that of generalized SSH theory, the agreement with experimental results is achieved by using adjustable parameters. However, these parameters have been fitted to experimental data only for low temperatures. A simple asymptotic formula proposed by Nikitin and Osipov [48], which expresses FHO transition probabilities for collisions with a small resonance defect in terms of Bessel functions, can also be useful for numerical simulations. This model permits one to avoid a singularity in transition probability calculations and noticeably saves computational time.

In Fig. 1 the rate coefficients of the VT transitions $\mathrm{CO}(X\ ^1\Sigma,i)+\mathrm{CO}\rightarrow \mathrm{CO}(X\ ^1\Sigma,i')+\mathrm{CO}$, calculated by means of different approaches, are given as functions of temperature. Transitions between low $(1\rightarrow 0)$ and high $(20\rightarrow 19)$ quantum states are considered. One can see that the best agreement with the trajectory calculations of Cacciatore and Billing [45] is achieved by using the FHO model [21] and the Nikitin and Osipov [48] formula (the results of these models practically coincide in the whole temperature range). The SSH model is not sufficiently precise for the two cases considered, while the approximation of Deleon and Rich [4] works well only for low temperatures. Similar results have been obtained for the probabilities of VV exchanges. In the latter case, the best agreement with trajectory calculations is given by the FHO model; the Nikitin model overestimates the probabilities of VV transitions between widely separated quantum states (i.e., transitions with a high resonance defect, for which the asymptotic solution is not correct). However, as shown in the next section, the contribution of VV processes (even when overestimating their probabilities) to high temperature CO vibrational kinetics is rather weak. Therefore, the Nikitin model, which represents a quite good accuracy/simplicity ratio, can be recommended for numerical

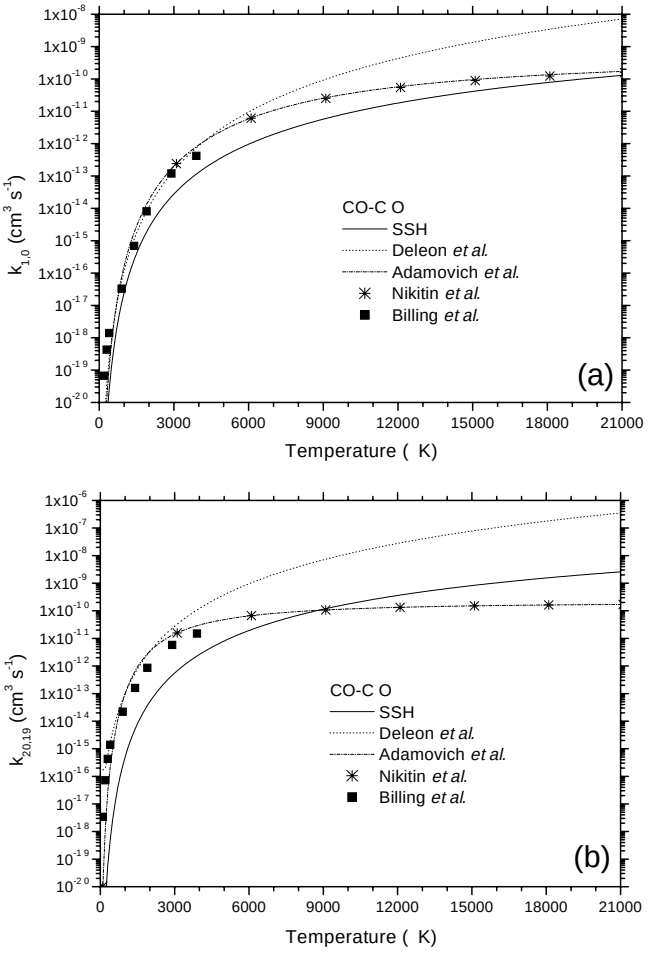

FIG. 1. Rate coefficients of VT transitions ($k_{ii'}$, $\mathrm{cm^3\,s^{-1}}$) in collisions with CO molecules. Temperature dependence calculated for different models. (a) transition $1\rightarrow 0$; (b) transition $20\rightarrow 19$.

simulations of high temperature CO flows. The results obtained using the SSH and Nikitin models are discussed in the next section.

Dissociation-recombination reaction rates can also be simulated using different models. The most reliable data on state-to-state dissociation rate coefficients are given by the quasiclassical dynamical approach (see, for instance, [17] for nitrogen dissociation rates). Unfortunately, this method consumes a lot of computational time. The simplest analytical model for dissociation rates is the ladder climbing model, based on the assumption that molecules dissociate through the last level, and each molecule reaching this level dissociates immediately with a probability equal to unity. The dissociation rate is thus determined by the stream of molecules from lower lying levels to the last level caused by VV and VT vibrational energy transitions. The Treanor-Marrone model [49] allows for dissociation from any vibrational level; in this case, state-to-state rate coefficients are connected to the thermal equilibrium rate coefficient by a nonequilibrium factor including an adjustable parameter U. Low values of this parameter correspond to preferential dissociation from high vibrational levels; $U=\infty$ describes nonpreferential dissociation from any level. A comparison of this model with the results of quasiclassical dynamical calculations given in [50] shows that in the general case the parameter U depends on the temperature and on the vibrational state of the molecule, especially at low temperatures and high vibrational levels. However, in the high temperature range, setting U equal to a fraction of the dissociation energy or $U=3T$ leads to a satisfactory agreement with quasiclassical calculations for all quantum states. The Treanor-Marrone model is used for further calculations of dissociation rate coefficients. Rate coefficients for VE transitions are taken from [4,6].

Production terms due to radiation R_ν^{rad} in Eqs. (15) for each transition $(\alpha ij\rightarrow\alpha' i' j')$ are found in the form

$$R_\nu^{rad}=h\nu[n_{\alpha ij}a_{\nu,\alpha ij\alpha' i' j'}+(n_{\alpha ij}b_{\nu,\alpha ij\alpha' i' j'} - n_{\alpha' i' j'}b_{\nu,\alpha' i' j'\alpha ij})I_\nu]. \tag{35}$$

Here the coefficients $b_{\alpha' i' j'\alpha ij}$, $b_{\alpha ij\alpha' i' j'}$, $a_{\alpha ij\alpha' i' j'}$ are the Einstein coefficients for absorption and induced and spontaneous emission, respectively. They are related by the detailed balance principle:

$$s_{j'}^{\alpha' i'}b_{\nu,\alpha' i' j'\alpha ij}=s_j^{\alpha i}b_{\nu,\alpha ij\alpha' i' j'}, \tag{36}$$

$$\frac{a_{\nu,\alpha ij\alpha' i' j'}}{b_{\nu,\alpha ij\alpha' i' j'}}=\frac{2h\nu^3}{c^2}. \tag{37}$$

Einstein coefficients can be calculated using the method described, for instance, in [51,52].

The production term due to radiation in Eqs. (11) can be written as

$$\begin{aligned}R_{\alpha i}^{rad}=&\sum_{\alpha'<\alpha}\sum_{i'}\sum_{j,j'}\int_0^\infty\int_{4\pi}[-n_{\alpha ij}a_{\nu,\alpha ij\alpha' i' j'}\\&+(n_{\alpha' i' j'}b_{\nu,\alpha' i' j'\alpha ij}-n_{\alpha ij}b_{\nu,\alpha ij\alpha' i' j'})I_\nu]d\nu d\boldsymbol{\Omega}_\nu\\&-\sum_{\alpha''>\alpha}\sum_{i''}\sum_{j,j''}\int_0^\infty\int_{4\pi}[-n_{\alpha'' i'' j''}a_{\nu,\alpha'' i'' j''\alpha ij}\\&+(n_{\alpha ij}b_{\nu,\alpha ij\alpha'' i'' j''}-n_{\alpha'' i'' j''}b_{\nu,\alpha'' i'' j''\alpha ij})I_\nu]d\nu d\boldsymbol{\Omega}_\nu\end{aligned} \tag{38}$$

with $\alpha'=\alpha=\alpha''$ and $i'<i<i''$ for transitions within the same electronic state.

These expressions can be simplified by introducing integral Einstein coefficients:

$$a_{\nu,\alpha ij\alpha' i' j'}=A_{\alpha ij\alpha' i' j'}\phi_{\nu,\alpha ij\alpha' i' j'}, \tag{39}$$

$$b_{\nu,\alpha ij\alpha' i' j'}=B_{\alpha ij\alpha' i' j'}\phi_{\nu,\alpha ij\alpha' i' j'}, \tag{40}$$

where $\phi_{\nu,\alpha ij\alpha' i' j'}$ is the line shape factor satisfying the normalizing condition

$$\int_0^\infty\phi_{\nu,\alpha ij\alpha' i' j'}d\nu=1. \tag{41}$$

Integral coefficients describe the probabilities of all radiative transitions that contribute to the transition $(\alpha ij \rightarrow \alpha' i' j')$. With the assumption that I_ν and $h\nu$ are slowly varying functions of frequency over the linewidth, integral Einstein coefficients are related by expressions similar to Eqs. (36) and (37) with ν corresponding to the center of the line.

Finally, simplified expressions for $R_{\alpha i}^{rad}$ have been derived, taking into account the isotropic character of the radiation field, the existence of the Boltzmann distribution over rotational energy, and normalizing conditions for the Hönl-London factors [40]:

$$R_{\alpha i}^{rad} = 4\pi \sum_{\alpha' < \alpha} \sum_{i'} \int_0^\infty \Phi_{\nu,\alpha i \alpha' i'} [-n_{\alpha i} A_{\alpha i \alpha' i'} + (n_{\alpha' i'} B_{\alpha' i' \alpha i} - n_{\alpha i} B_{\alpha i \alpha' i'}) I_\nu] d\nu - 4\pi \sum_{\alpha'' > \alpha} \sum_{i''} \int_0^\infty \Phi_{\nu,\alpha'' i'' \alpha i} [-n_{\alpha'' i''} A_{\alpha'' i'' \alpha i} + (n_{\alpha i} B_{\alpha i \alpha'' i''} - n_{\alpha'' i''} B_{\alpha'' i'' \alpha i}) I_\nu] d\nu, \quad (42)$$

where $\Phi_{\nu,\alpha i \alpha' i'}$ is the band profile function [53] satisfying the normalizing condition

$$\int_0^\infty \Phi_{\nu,\alpha i \alpha' i'} d\nu = 1. \quad (43)$$

Data for the calculation of the integral Einstein coefficients $A_{\alpha i \alpha' i'}$, $B_{\alpha i \alpha i'}$, and $B_{\alpha' i' \alpha i}$ for absorption and induced and spontaneous emission, respectively, can be found in [6,54].

At this point, one can see that in Eqs. (11)–(15), vibrational relaxation, dissociation, and radiative transitions are completely coupled; the radiative production terms are calculated without using the general assumption about local thermal equilibrium. A similar approach has been considered in [4,6,9] for the simple case of a motionless gas in a laser cell. In the next section a gas flow behind a shock wave is studied numerically on the basis of this model.

IV. RESULTS AND DISCUSSION

In this section, a nonequilibrium CO flow behind a shock wave is investigated in the following free-stream conditions: $v_0 = 5200$ m/s, $T_0 = 300$ K, $p_0 = 500$ Pa, which correspond to a Mach number of about 15. Since the pressure behind the shock is about atmospheric, a Doppler profile is chosen for the line shape factor simulation. Initial vibrational distributions of the CO molecules are supposed to be in equilibrium at temperature T_0. Equations (11)–(15) have been resolved using the Gear method for the solution of stiff ordinary differential equation systems.

First let us discuss the influence of VV transitions on vibrational distributions and macroscopic parameters. Figure 2 represents the evolution of CO vibrational level populations behind the shock, calculated taking into account VV+VT and only VT processes. State-to-state distributions have been obtained using the Nikitin model. One can note a small discrepancy in the populations of high quantum states at x about 0.01–0.1 cm behind the shock front; this difference disappears at shorter distances and with rising x. The discrepancy might be caused by a tendency of the Nikitin model to overestimate VV rates of transitions between widely separated states. When using the SSH model for vibrational exchange rates, the influence of VV transitions on vibrational distributions is practically negligible. For both models, the gas temperature and other macroscopic parameters are completely insensitive to neglect of VV transitions. This fact is very encouraging, because the calculation of VV rate coefficients is one of the most time consuming procedures. Thus one can eliminate VV processes when studying high temperature CO kinetics, which is not the case in low temperature optically pumped systems.

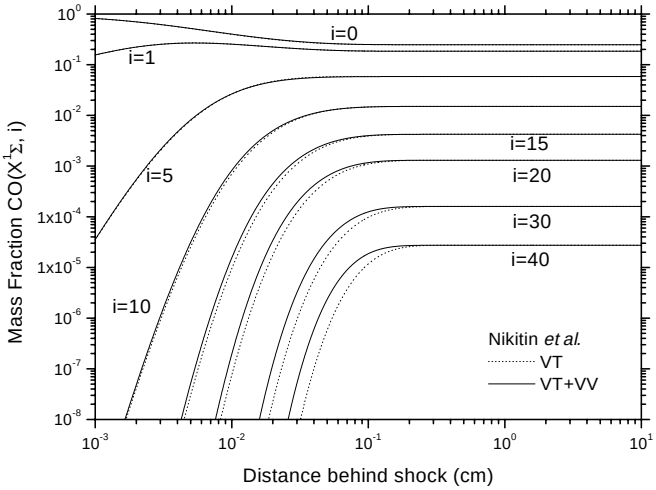

FIG. 2. Evolution of vibrational level populations behind the shock front. $v_0 = 5200$ m/s, $T_0 = 300$ K, $p_0 = 500$ Pa. Influence of VV exchanges.

In Fig. 3 the evolution of level populations calculated using the SSH and Nikitin models is given. While for low levels the two models lead to similar results, for intermediate and high levels the difference is significant. The SSH model

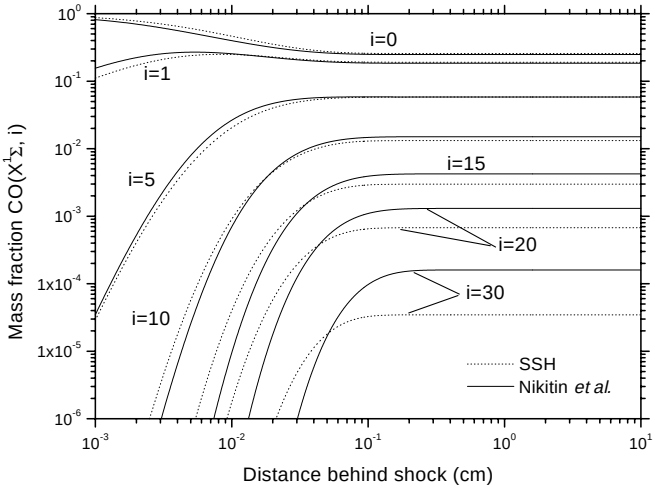

FIG. 3. Evolution of vibrational level populations behind the shock front. $v_0 = 5200$ m/s, $T_0 = 300$ K, $p_0 = 500$ Pa. Comparison of SSH and Nikitin models.

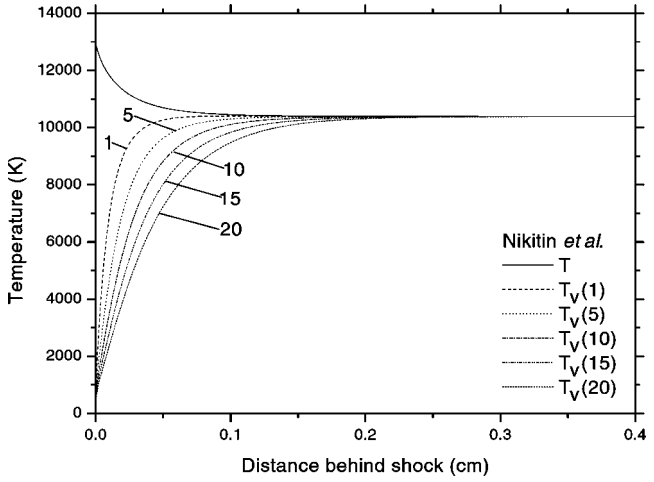

FIG. 4. Vibrational temperature of different levels as a function of x. $v_0=5200$ m/s, $T_0=300$ K, $p_0=500$ Pa.

overestimates the rate of VT transitions between highly located states, and thus leads to a more rapid population of high levels. However, equilibrium values of populations of high quantum states are lower compared to the ones given by the model of Nikitin. Moreover, it has been found that the SSH theory developed for harmonic oscillators, provides Boltzmann-like distributions whereas the models taking into account anharmonicity of vibrations give distributions deviating from the Boltzmann one. This can be seen from Fig. 4, where vibrational temperatures of different levels introduced by the definition

$$T_v(\alpha,i)=\frac{1}{k}\,\frac{\varepsilon_{\alpha i}-\varepsilon_{\alpha i-1}}{\ln(n_{\alpha i}/n_{\alpha i-1})} \tag{44}$$

($\varepsilon_{\alpha i}$ is the vibrational energy of the ith level of the electronic state α) are plotted. One can see that the vibrational temperatures of various states differ noticeably and reach equilibrium at different times. This seems to be a serious argument against the validity of multitemperature models for harmonic oscillators based on the assumption of a single vibrational temperature for all vibrational levels.

Figures 5 and 6 demonstrate the influence of dissociation on vibrational distributions. Taking into account the dissociation process dramatically changes the shape of distributions at $x>0.01$ cm behind the shock because of the depletion of high quantum states. The choice of the parameter $U=3T$ or $U=\vartheta_{diss}/6$ (ϑ_{diss} is the dissociation energy in kelvin) weakly affects the shape of distributions, whereas the value $U=\vartheta_{diss}/20$, which corresponds to preferential dissociation from very high levels, gives a different distribution shape, with higher population of intermediate levels and sharp decrease of the distribution tail population. In the case of nonpreferential dissociation ($U=\infty$), Boltzmann-like distributions have been found.

It is interesting to emphasize the very weak influence of VE processes on the vibrational distributions. It is well known that in low temperature CO systems VE transitions lead to a crucial depletion of the states close to $i=26$ and $i=40$, which are almost isoenergetic with the first and second

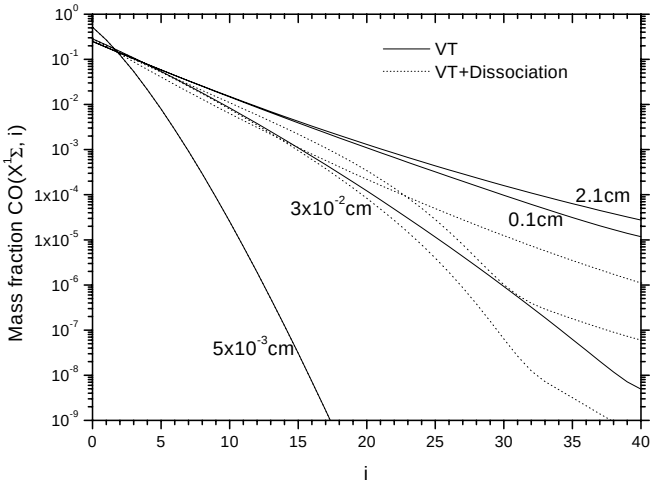

FIG. 5. Vibrational distributions as functions of i at various distances from the shock front. $v_0=5200$ m/s, $T_0=300$ K, $p_0=500$ Pa. Contribution of the dissociation process.

CO electronic states [4–6]. In the high temperature case, the rate of dissociation from the upper vibrational states appears to be much higher than the rate of VE transitions, and thermal decomposition of CO molecules becomes dominant compared to VE transitions from the ground electronic state. This can be seen in Fig. 7, which presents the evolution of the CO 40th level population behind the shock, taking into account successively the VT, VE, and dissociation processes.

The effect of dissociation and various models of vibrational transition rates on the gas temperature behind the shock is demonstrated in Fig. 8. It is not surprising that taking into account thermal dissociation provides a significant decrease of the equilibrium gas temperature attained at the end of the relaxation zone. When dissociation is neglected, thermal equilibrium is established at a considerably shorter distance from the shock front, and an important energy supply, which could be spent in the dissociation reaction, is retained in the translational mode. One can see also that using

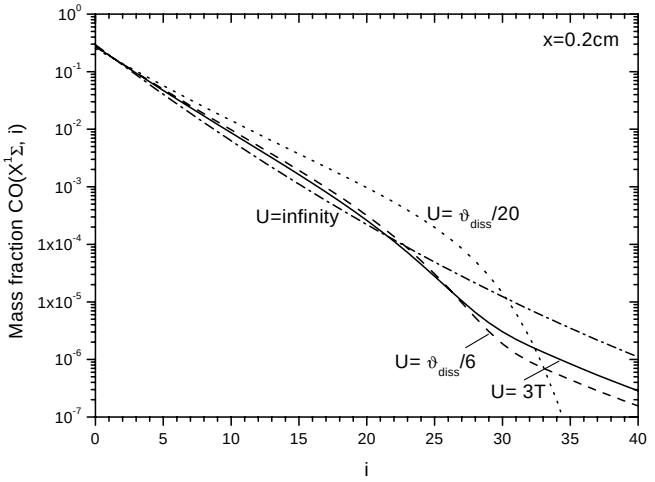

FIG. 6. Vibrational distributions as functions of i at $x=0.2$ cm. $v_0=5200$ m/s, $T_0=300$ K, $p_0=500$ Pa. Influence of the parameter U.

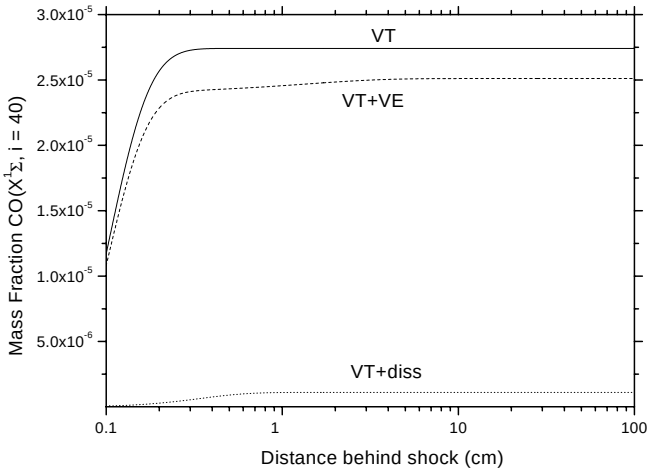

FIG. 7. Mass fraction of the 40th CO vibrational level as a function of x. $v_0=5200$ m/s, $T_0=300$ K, $p_0=500$ Pa. Contribution of VE and dissociation processes.

the SSH model leads to a slower decrease of the gas temperature. At the present initial conditions, the SSH theory underestimates rates of VT transitions at low vibrational levels, which are responsible for gas temperature values. Since the excitation rate of the first vibrational states is lower in this case, thermal equilibrium for the SSH model is achieved later, especially when dissociation is taken into account.

Figure 9 presents atomic molar fractions as functions of the distance from the shock front, calculated using different models for the rates of vibrational transitions and dissociation. For nonpreferential dissociation ($U=\infty$), chemical equilibrium is attained faster than in the preferential dissociation model. The influence of the model of VT transition rates on the atom formation rate is rather weak in this case; both SSH and Nikitin models give similar results. This can be explained by the fact that in the nonpreferential case dissociation may proceed from any vibrational level, in particular, from highly populated low levels. Since the SSH and Nikitin models provide practically the same results for low

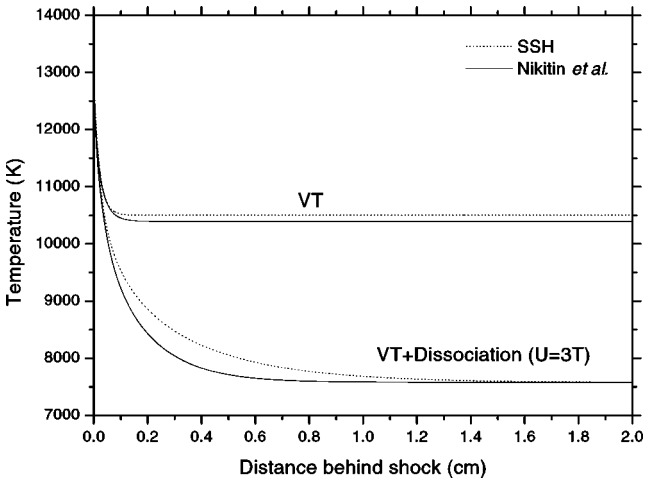

FIG. 8. Gas temperature as a function of x. $v_0=5200$ m/s, $T_0=300$ K, $p_0=500$ Pa. Influence of dissociation and different models for VT transition rates.

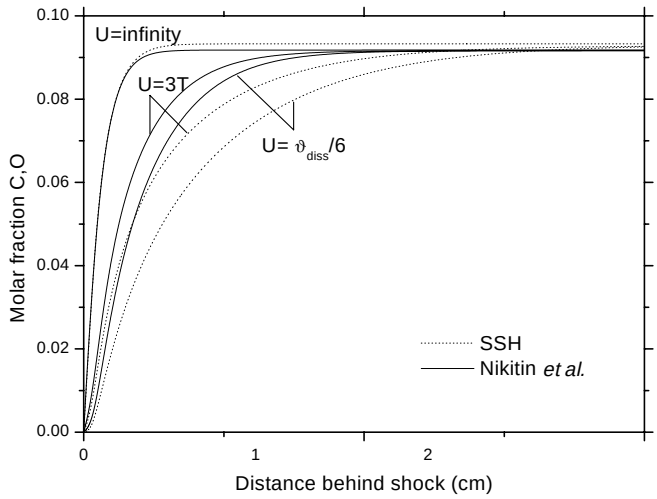

FIG. 9. Molar fraction of atoms as a function of x. $v_0=5200$ m/s, $T_0=300$ K, $p_0=500$ Pa. Influence of dissociation and VT transition rates.

level populations (Fig. 3), rates of atom formation are very close for both these models. In contrast, for preferential dissociation, the behavior of the upper vibrational levels is of importance. As populations of upper levels obtained using the SSH and Nikitin models vary considerably, the rates of atomic species formation are also different. Thus the SSH model, which gives a lower population of high levels at $x>0.1$ cm (see Fig. 3), provides a lower rate of preferential dissociation.

Let us discuss now the features of VE transitions and radiation. Vibration-to-electronic transitions lead to the formation of electronically excited states (CO $a\ ^3\Pi$ and $A\ ^1\Pi$ states are considered). Then electronically excited particles, whose radiative lifetime is usually short (about several nanoseconds [6]), descend to the ground state, emitting photons in the uv range. The influence of dissociation and radiation processes on the mass fractions of $a\ ^3\Pi$ and $A\ ^1\Pi$ states is demonstrated in Figs. 10 and 11. Dissociation diminishes the population of high vibrational levels of the ground electronic state, thus making VE transitions from upper vibrational states less efficient, which explains the significant decrease of excited state populations (see Fig. 10 for the $a\ ^3\Pi$ state; similar results are obtained for the $A\ ^1\Pi$ state). Taking into account uv radiation from the fourth positive system also considerably decreases populations of the $A\ ^1\Pi$ state due to radiative decay. Figure 11 gives results for $A\ ^1\Pi$. Note that all collision processes, VT, VE, and dissociation, are included now in the kinetic scheme. While the effect of uv radiation on electronic state populations is found to be important, the influence of ir radiation on vibrational level populations of the $X\ ^1\Sigma$ state is practically negligible. The reason for that probably lies in the comparatively long radiative lifetime of excited vibrational levels of $X\ ^1\Sigma$ state (about several milliseconds). It should be noted also that the influence of both ir and uv radiative processes on macroscopic flow parameters (gas temperature, pressure, velocity) is found to be very weak.

Figure 12 presents the intensity of ir and uv radiation

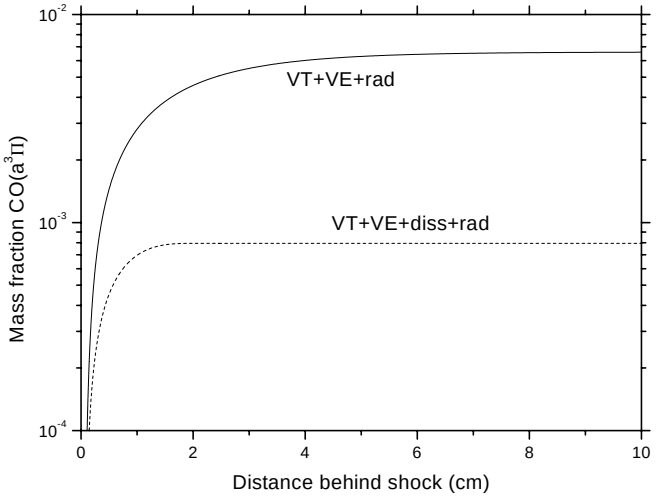

FIG. 10. Mass fraction of CO $a\ ^3\Pi$ excited state as a function of x. $v_0=5200$ m/s, $T_0=300$ K, $p_0=500$ Pa. Influence of dissociation.

calculated using the complete kinetic scheme and also neglecting dissociation. It is seen that thermal dissociation strongly affects radiative processes, significantly decreasing both ir and uv radiation intensity.

The effect of VT transition rates on the radiation intensity is shown in Fig. 13. The complete kinetic scheme including all collision and radiative processes is applied here. One can see a weak influence of the VT transition probabilities on the ir radiation intensity. At the same time, uv and total intensities are considerably affected by the rate of the VT process. This is caused by the different rate of population of high vibrational levels, which provide a source of electronically excited states responsible for uv radiation.

Figure 14 presents a comparison of the ir radiation intensity [the band corresponding to the (2,1) vibrational transition] behind a shock wave calculated by means of the detailed nonequilibrium model developed in the present paper

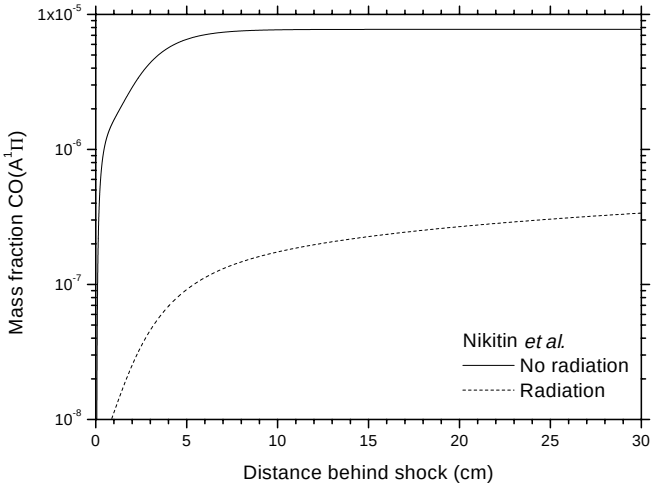

FIG. 11. Mass fraction of CO $A\ ^1\Pi$ excited state as a function of x. $v_0=5200$ m/s, $T_0=300$ K, $p_0=500$ Pa. Influence of radiation.

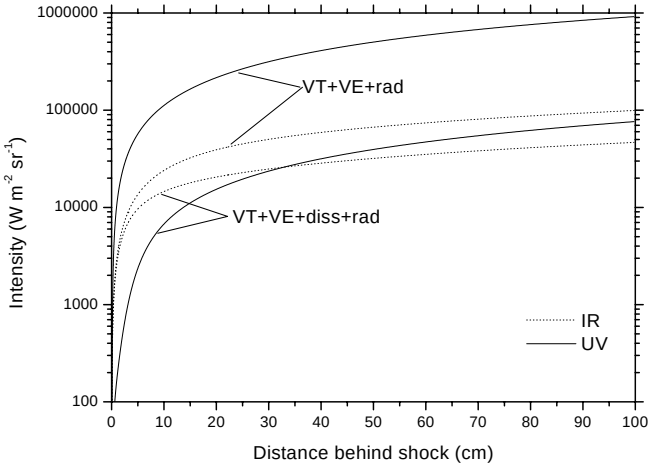

FIG. 12. Radiation intensity as a function of x. $v_0=5200$ m/s, $T_0=300$ K, $p_0=500$ Pa. Influence of dissociation.

and for thermochemical equilibrium conditions (using the Planck function for blackbody radiation). A great discrepancy of results in the nonequilibrium region is found. One can conclude that the assumption of thermal and chemical equilibrium for calculation of the radiative heat flux in real gas flows can lead to a significant error.

The mixture composition behind the shock front calculated taking into account all considered processes (except VV exchanges, whose contribution to the high temperature CO kinetics is shown to be negligibly small) is given in Fig. 15. One can see a weak degree of dissociation as well as low concentrations of electronically excited molecules. Nevertheless, with increasing distance from the shock front, even low populations of excited electronic states provide a greater uv radiation intensity compared to the ir intensity. A similar low dissociation degree in a shock heated CO flow was found in [55].

V. CONCLUSIONS

A nonequilibrium high temperature radiative CO flow behind a strong shock wave has been studied using the detailed

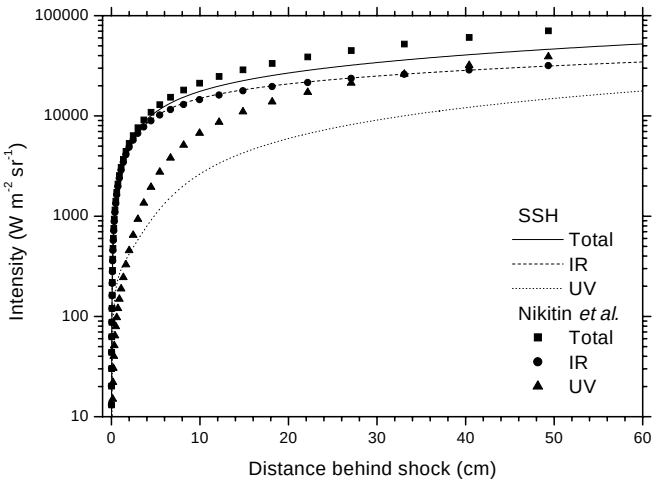

FIG. 13. Radiation intensity as a function of x. $v_0=5200$ m/s, $T_0=300$ K, $p_0=500$ Pa. Influence of VT transition rates.

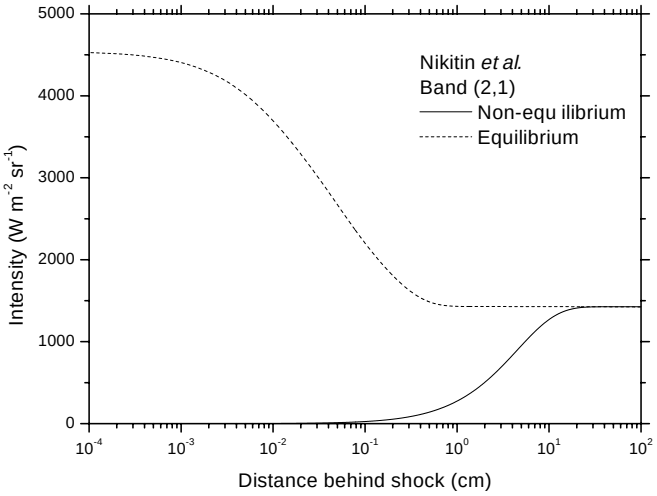

FIG. 14. ir radiation intensity as a function of x. $v_0 = 5200$ m/s, $T_0 = 300$ K, $p_0 = 500$ Pa. Comparison of equilibrium and nonequilibrium intensity distributions.

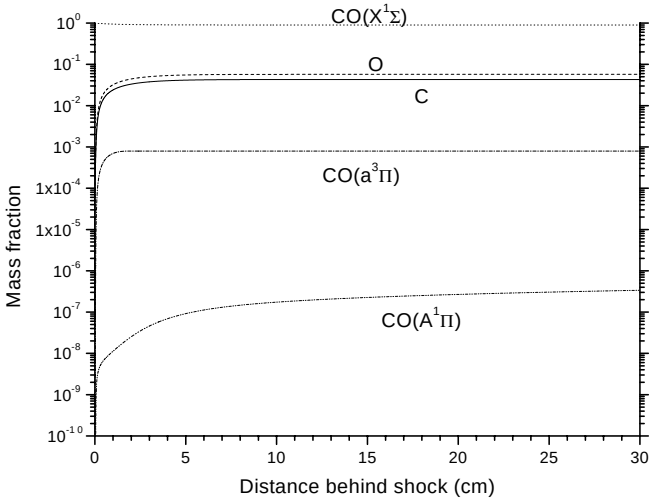

FIG. 15. Mass fractions of all species as functions of x. $v_0 = 5200$ m/s, $T_0 = 300$ K, $p_0 = 500$ Pa. Complete kinetic scheme.

self-consistent state-to-state kinetic theory approach. Various collision processes (VV, VT, VE transitions, dissociation) as well as ir and uv radiation processes have been included successively in the kinetic scheme. The contribution of these processes to the formation of vibrational distributions and to the evolution of macroscopic flow parameters has been investigated. The main processes affecting the gas temperature, pressure, and velocity are VT excitation and dissociation. The influence of VV and VE exchanges and radiation on these macroscopic parameters is found to be negligible. However, VE transitions provide a source of electronically excited molecules and thus contribute significantly to the uv emission intensity.

Different models of vibrational transition probabilities and dissociation rates have been tested. One can conclude that the simple asymptotic formula of Nikitin and Osipov for VT transition rates has good accuracy and can be successfully used in numerical simulation of CO flows.

Finally, for further improvement of the model developed, one should include exchange reactions with formation of C_2 molecules in the kinetic scheme. Although exchange reactions will complicate the model considerably, it will give a good opportunity to study radiation of the Swan system (which is usually observed in shock tube experiments), and thus will enable us to validate the model experimentally.

ACKNOWLEDGMENTS

This work is partially supported by the Russian Foundation for Basic Research (Project No. 02-03-42044). The University of Provence and CNRS supported visits of E.K. to IUSTI (University of Provence).

[1] J. Rich and R. Bergman, Chem. Phys. **44**, 53 (1979).
[2] S. De Benidictis, F. Cramarossa, and R. D'Agostino, Chem. Phys. **82**, 395 (1983).
[3] C. Gorse, M. Cacciatore, and M. Capitelli, Chem. Phys. **85**, 165 (1984).
[4] R. Deleon and J. Rich, Chem. Phys. **107**, 283 (1986).
[5] R. Farrenq, C. Rosetti, G. Guelachvili, and W. Urban, Chem. Phys. **92**, 389 (1985).
[6] C. Flament, T. George, K. Meister, J. Tufts, J. Rich, V. Subramanian, J.-P. Martin, B. Piar, and M.-Y. Perrin, Chem. Phys. **163**, 241 (1992).
[7] Y. Ionikh, I. Kostyukevich, and N. Chernysheva, Opt. Spectrosc. **76**, 361 (1994).
[8] H. Wallaart, B. Piar, M.-Y. Perrin, and J.-P. Martin, Chem. Phys. **196**, 149 (1995).
[9] E. Plönjes, P. Palm, A. Chernukho, I. Adamovich, and J. Rich, Chem. Phys. **256**, 315 (2000).
[10] A. Fairbairn, Proc. R. Soc. London, Ser. A **312**, 207 (1969).
[11] J. Appleton, M. Steinberg, and D. Liquornik, J. Chem. Phys. **52**, 2205 (1970).
[12] R. Hanson, J. Chem. Phys. **60**, 4970 (1974).
[13] O. Brandt and P. Roth, Phys. Fluids **30**, 1294 (1987).
[14] G. Billing and E. Fisher, Chem. Phys. **43**, 395 (1979).
[15] G. Billing and R. Kolesnick, Chem. Phys. Lett. **200**, 382 (1992).
[16] G. Billing, in *Nonequilibrium Vibrational Kinetics*, edited by M. Capitelli (Springer-Verlag, Berlin, 1986), pp. 85–111.
[17] F. Esposito, M. Capitelli, and C. Gorse, Chem. Phys. **257**, 193 (2000).
[18] F. Esposito and M. Capitelli, Chem. Phys. Lett. **302**, 49 (1999).
[19] E. Nagnibeda, in *Aerothermodynamics for Space Vehicles*, edited by J. Hunt (ESA Publication Division, ESTEC, Noordwijk, The Netherlands, 1995).
[20] F. Lordet, J. Meolans, A. Chauvin, and R. Brun, Shock Waves **4**, 299 (1995).
[21] I. Adamovich, S. Macheret, J. Rich, and C. Treanor, AIAA J. **33**, 1064 (1995).
[22] S. Ruffin and C. Park, AIAA Pap. **92**, 0806 (1992).
[23] A. Chiroux de Gavelle de Roany, C. Flament, J. Rich, V. Sub-

ramaniam, and W. Warren, Jr., AIAA J. **31**, 119 (1993).
[24] B. Shizgal and F. Lordet, J. Chem. Phys. **104**, 3579 (1996).
[25] G. Colonna, M. Tuttafesta, M. Capitelli, and D. Giordano, in *Rarefied Gas Dynamics 21* (CEPADUES, Toulouse, France, 1999), Vol. 2, pp. 281–288.
[26] I. Armenise, M. Capitelli, G. Colonna, and C. Gorse, J. Thermophys. Heat Transfer **10**, 397 (1996).
[27] M. Capitelli, I. Armenise, and C. Gorse, J. Thermophys. Heat Transfer **11**, 570 (1997).
[28] G. Candler, J. Olejniczak, and B. Harrold, Phys. Fluids **9**, 2108 (1997).
[29] E. Kustova and E. Nagnibeda, Chem. Phys. **233**, 57 (1998).
[30] E. Kustova and E. Nagnibeda, in *Rarefied Gas Dynamics 21* [25], Vol. 1, pp. 231–238.
[31] I. Armenise, M. Capitelli, E. Kustova, and E. Nagnibeda, J. Thermophys. Heat Transfer **13**, 210 (1999).
[32] M. Capitelli, G. Colonna, D. Giordano, E. Kustova, E. Nagnibeda, M. Tuttafesta, and D. Bruno, Math. Modell. **11**, 45 (1999).
[33] V. Zhigulev, Inzh. Zh. **4**, 231 (1964) (in Russian).
[34] J. Arnold, V. Reis, and H. Woodward, AIAA Pap. **65**, 0166 (1965).
[35] V. Agafonov, V. Vertushkin, A. Gladkov, and O. Polyanskii, *Nonequilibrium Physical and Chemical Processes in Aerodynamics* (Mashinostroenie, Moscow, 1972) (in Russian).
[36] C. Park, *Nonequilibrium Hypersonic Aerothermodynamics* (Wiley and Sons, New York, 1990).
[37] G. Candler and C. Park, AIAA Pap. **88**, 2678 (1988).
[38] E. Kustova and A. Chikhaoui, Chem. Phys. **255**, 59 (2000).
[39] E. Kustova, A. Aliat, and A. Chikhaoui, Chem. Phys. Lett. **344**, 638 (2001).
[40] A. Aliat, Ph.D. thesis, Université de Provence, 2002.
[41] C.S. Wang Chang and G. Uhlenbeck, University of Michigan Research Report No. cm-681, 1951 (unpublished).
[42] G. Ludwig and M. Heil, in *Advances in Applied Mechanics* (Academic Press, New York, 1960), Vol. VI.
[43] A. Chikhaoui, J. Dudon, E. Kustova, and E. Nagnibeda, Physica A **247**, 526 (1997).
[44] P. Brechignac, Chem. Phys. **34**, 119 (1978).
[45] M. Cacciatore and G. Billing, Chem. Phys. **58**, 395 (1981).
[46] R. Schwartz, Z. Slawsky, and K. Herzfeld, J. Chem. Phys. **20**, 1591 (1952).
[47] B. Gordiets, A. Osipov, and L. Shelepin, *Kinetic Processes in Gases and Molecular Lasers* (Gordon and Breach Science Publishers, Amsterdam, 1988).
[48] E. Nikitin and A. Osipov, in *Kinetics and Catalysis* (VINITI, All-Union Institute of Scientific and Technical Information, Moscow, 1977), Vol. 4, Chap. 2 (in Russian).
[49] P. Marrone and C. Treanor, Phys. Fluids **6**, 1215 (1963).
[50] F. Esposito, M. Capitelli, E. Kustova, and E. Nagnibeda, Chem. Phys. Lett. **330**, 207 (2000).
[51] G. Herzberg, *Infrared and Raman Spectra of Polyatomic Molecules* (Van Nostrand Company, New York, 1951).
[52] M. Mitchner and C. Kruger, *Partially Ionized Gases*, Wiley Series in Plasma Physics (Wiley and Sons, New York, 1973).
[53] S. Gilles and W. Vincenti, J. Quant. Spectrosc. Radiat. Transf. **10**, 71 (1970).
[54] H. Heaps and G. Herzberg, Z. Phys. **133**, 49 (1953).
[55] D. Ramjaun, Ph.D. thesis, Université de Provence, Marseille, France, 1999.